COMMUN. MATH. SCI.
Vol. 13, No. 5, pp. 1289–1315

DYNAMIC TRANSITIONS AND PATTERN FORMATIONS FOR A CAHN–HILLIARD MODEL WITH LONG-RANGE REPULSIVE INTERACTIONS*

HONGHU LIU†, TAYLAN SENGUL‡, SHOUHONG WANG§, AND PINGWEN ZHANG¶

Abstract. The main objective of this article is to study the order-disorder phase transition and pattern formation for systems with long-range repulsive interactions. The main focus is on a Cahn–Hilliard model with a nonlocal term in the corresponding energy functional, representing certain long-range repulsive interaction. We show that as soon as the trivial steady state loses its linear stability, the system always undergoes a dynamic transition of one of three types — continuous, catastrophic and random — forming different patterns/structures, such as lamellae, hexagonally packed cylinders, rectangles, and spheres. The types of transitions are dictated by a non-dimensional parameter, measuring the interactions between the long-range repulsive term and the quadratic and cubic nonlinearities in the model. In particular, the hexagonal pattern is unique to this long-range interaction, and it is captured by the corresponding two-dimensional reduced equations on the center manifold, which involve (degenerate) quadratic terms and non-degenerate cubic terms. Explicit information on the metastability and basins of attraction of different ordered states, corresponding to different patterns, are derived as well.

Key words. Phase transition, pattern formation, long-range interaction, a Cahn–Hilliard model, center manifold reduction, hexagonal pattern.

AMS subject classifications. 35B32, 35B36, 37L05, 37L10.

1. Introduction

Many systems in nature can be modeled through the inclusion of long-range interactions, examples include uniaxial ferromagnetic films, Langmuir monolayers, block copolymers, and cholesteric liquid crystals; see, e.g., Desai and Kapral [8, Chap. 13] and references therein. The competition between long-range repulsive interactions and short-range attractive interactions leads to new features that are not present in systems with only short range interactions [8, 23].

The main objective of this article is to study the order-disorder phase transition and pattern formation of binary systems confined in a bounded domain with long-range and short-range interaction competitions, and to analyze the effects of the long-range repulsive interactions on the phase transition. In particular, the transitions from disordered state to lamellae (LAM), hexagonally packed cylinders (HPC), rectangles, and spheres are explored.

The energy functional we adopt in this article is derived by adding a nonlocal term to the usual Cahn–Hilliard free energy functional [4], measuring the long-range repulsive interactions; see (2.1) below. It is also known as the Ohta–Kawasaki functional in the diblock copolymer context [6, 7, 18, 20]. We refer the interested readers to [8, 22] for models involving more general long-range terms.

The mathematical analysis of the model is carried out using techniques from dynamic transition theory developed recently by Ma and Wang [14, 16]; see also Appendix A for a brief account of this theory. The main philosophy of dynamic transition

*Received: Nobember 8, 2012; accepted (in revised form): August 29, 2014. Communicated by John Lowengrub.

†Department of Atmospheric & Oceanic Sciences, University of California, Los Angeles, CA 90095-1565, USA (hliu@atmos.ucla.edu).

‡Department of Mathematics, Yeditepe University, Istanbul, Turkey (taylansengul@gmail.com).

§Department of Mathematics, Indiana University, Bloomington, IN 47405, USA (showang@indiana.edu, http://www.indiana.edu/fluid).

¶Department of Mathematics, Beijing University, Beijing, P.R. China (pzhang@pku.edu.cn).

theory is to search for the full set of transition states, leading to a complete characterization of stability and transition. The set of transition states is often represented by a local attractor. Following this idea, the theory is developed to identify the transition states and to classify them both dynamically and physically.

One important ingredient of the theory is a new classification scheme of transitions, in which phase transitions are classified into three types: Type-I, Type-II and Type-III. In more mathematically intuitive terms, they are called continuous, catastrophic, and random transitions, respectively. Basically, as the control parameter passes the critical threshold, the transition states stay in a close neighborhood of the basic state for a Type-I transition; and they are outside of a neighborhood of the basic state for a Type-II transition. For a Type-III transition, a neighborhood of the basic state is divided into two open regions with a Type-I transition in one region, and a Type-II transition in the other region; cf. Theorem A.1.

We describe now the main results of this article. The related physical significance is also briefly mentioned, and more detailed physical conclusions are left for future work.

First, we show that as soon as the trivial steady state loses its linear stability, the system always undergoes a transition of one of the aforementioned three types, forming different patterns/structures. The type of transition is dictated by a non-dimensional parameter, measuring the interactions between a linear term σu, originated from the long-range repulsive interactions, and the quadratic and cubic nonlinearities $\gamma_2\Delta u^2$, $\gamma_3\Delta u^3$ in the model Equation (2.6) below. For example, in the LAM case analyzed in Theorem 4.1, this parameter is given by

$$\mathcal{B} \simeq \gamma_3 - \frac{8}{27}\frac{\gamma_2^2}{\sqrt{\sigma}},$$

where $\mathcal{B} > 0$ indicates first order transitions, and $\mathcal{B} < 0$ implies second-order transitions; see (4.1) for the exact formula of $\mathcal{B}$.

Second, the long-range interaction term $\frac{\sigma_d}{2}(-\Delta)^{-\frac{1}{2}}(u_A - a)\cdot(-\Delta)^{-\frac{1}{2}}(u_A - a)$ in the energy functional (2.1) below plays an essential role in pattern selection.[1] In particular, there are three unique features induced by this long-range interaction term, which are not present in the phase transition dynamics and pattern formations described by the classical Cahn–Hilliard model [15], where $\sigma_d = 0$. The first new feature is that the associated pattern selection mechanism here involves the long-range repulsive interaction parameter, σ_d, which leads to more possible patterns that are absent in the classical Cahn–Hilliard model; see (3.6). Moreover, the scale of the spatial patterns emerging from the transition is determined by the parameter σ_d. Finally, the long-range interaction causes the periodic structure emerging from the transition to be very sensitive to the system parameters; see again the pattern selection criterion (3.6).

Third, an important technical ingredient of the study is the reduction of the underlying partial differential equation (PDE) to its corresponding local center manifold. The resulting reduced equations that govern the local dynamics of the original PDE are analyzed carefully following the ideas of dynamic transition theory [14, 16]. Unlike many other dynamic transition problems we have encountered, in the HPC case, the reduced equations consist of (degenerate) quadratic terms and non-degenerate cubic terms. This unique feature of the reduced system is caused directly by the introduction of the long-range interaction term in the energy functional (2.1) below.

Fourth, in the HPC case, the transition can be of either Type-I or Type-II or Type-III. In the Type-III case, a neighborhood of the basic state is divided into two open

[1] Here, σ_d is the dimensional form of the parameter σ mentioned in the previous paragraph.

regions with a continuous transition in one region, and a jump transition in the other region. The HPC structures are located on the boundary of these two regions; see Theorem 4.2 (iii).

It is worth mentioning that dynamic transition theory enables us not only to derive precise information on the type of transitions and phase diagram, but also to obtain basins of attraction of different phases (fluctuations), which are otherwise unavailable; see, e.g., Theorem 4.2 below.

The article is organized as follows. In Section 2, a Cahn–Hilliard type equation incorporating long range interactions is introduced. The linear problem of this equation is presented in Section 3, and the phase transitions and pattern formations associated with the model are derived in Section 4. Section 5 is devoted to the proofs of the main theorems.

2. A Cahn–Hilliard model with long-range interactions

We consider an incompressible binary system with long-range repulsive interactions. Let u_A and u_B be the concentrations of components A and B, respectively. By the incompressibility of the system, $u_A+u_B=1$. Thanks to this identity, the free energy functional can be expressed in terms of u_A only, and it takes the following form:

$$\begin{aligned} F(u_A)=\int_\Omega \Big(&\frac{\mu}{2}|\nabla u_A|^2+f(u_A)\\ &+\frac{\sigma_d}{2}(-\Delta)^{-\frac{1}{2}}(u_A-a)\cdot(-\Delta)^{-\frac{1}{2}}(u_A-a)\Big)\,\mathrm{d}x+F_0, \end{aligned} \tag{2.1}$$

where $\Omega\subset\mathbb{R}^3$ is a bounded domain; the coefficients μ and σ_d are positive parameters; $(-\Delta)^{-1/2}$ is a fractional power of the Laplace operator under zero flux boundary condition; a is the concentration of component A in the disordered state, namely $a=\frac{1}{|\Omega|}\int_\Omega u_A(x)\,\mathrm{d}x$ with $|\Omega|$ being the volume of Ω; and F_0 is the energy of the system when it is in the disordered state (*i.e.,* when $u_A\equiv a$).

The term $\frac{\mu}{2}|\nabla u_A|^2$ in (2.1) represents the interfacial free energy. The term $f(u_A)$ measures the bulk energy of the mixing and usually takes a double well form. For simplicity, we assume that[2]

$$f(u_A)=b_1(u_A-a)^2+b_2(u_A-a)^3+b_3(u_A-a)^4,$$

where b_1, b_2 and b_3 are constants with $b_3>0$. The third term in (2.1) reflects long-range interactions with σ_d measuring the interaction strength; see [7, 18] for more details.

When $\sigma_d=0$, the energy functional (2.1) is reduced to the classical Cahn–Hilliard free energy functional [4]. It is worth mentioning that (2.1) is also known in the literature as a Ginzburg–Landau functional with competing or Coulomb-type interaction [17], or an Ohta–Kawasaki functional in the context of phase separation of diblock copolymers [20].

We turn now to present the governing equation associated with the energy functional (2.1). For this purpose, let

$$u:=u_A-a. \tag{2.2}$$

The equation governing the evolution of u can be derived as the gradient flow of the energy functional (2.1) under the $H^{-1}(\Omega)$ norm with a constant mobility factor. This

[2] As far as the dynamic transition is concerned, more general form of the nonlinearity can be dealt with by applying a Taylor expansion of the nonlinearity about the disordered state $u_A\equiv a$.

can be done in the same fashion as the derivation of the usual Cahn–Hilliard equation from the corresponding free energy functional; see, e.g., [6, 10, 12, 13, 19]. The equation reads:

$$\frac{\partial u}{\partial t} = m[-\mu\Delta^2 u + \Delta(b_1 u + b_2 u^2 + b_3 u^3) - \sigma_d u], \tag{2.3}$$

where $m > 0$ is the constant mobility, and other parameters are as mentioned above.

Equation (2.3) is supplemented with Neumann and no-flux boundary conditions:

$$\frac{\partial u}{\partial n} = 0, \quad \frac{\partial \Delta u}{\partial n} = 0 \text{ on } \partial\Omega; \tag{2.4}$$

and suitable initial condition $u(x,0) = \psi$. For simplicity, we consider the spatial domain to be a bounded rectangular domain, i.e., $\Omega = \prod_{i=1}^{3}(0, L_i^d)$.

Note that the quantity $\int_\Omega u(x,t)\,\mathrm{d}x$ is conserved, which can be checked by integrating both sides of Equation (2.3) over Ω, and applying the divergence theorem to the RHS and making use of the boundary condition (2.4). Now by integrating both sides of (2.2) over Ω and by noting that $a = \frac{1}{|\Omega|}\int_\Omega u_A(x)\,\mathrm{d}x$, we obtain the following mean-zero condition on u:

$$\int_\Omega u(x,t)\,\mathrm{d}x = 0. \tag{2.5}$$

Throughout this article, we will work with a non-dimensional form of (2.3). For this purpose, let us introduce the following non-dimensional variables and parameters:

$$x' = \frac{x}{d}, \qquad t' = \frac{m\mu}{d^4}t, \quad u' = u, \qquad \lambda = -\frac{d^2 b_1}{\mu},$$
$$\gamma_2 = \frac{d^2 b_2}{\mu}, \quad \gamma_3 = \frac{d^2 b_3}{\mu}, \quad \sigma = \frac{d^4}{\mu}\sigma_d,$$

where d is a typical length scale related to the domain Ω. Then, the system (2.3)–(2.5) can be recast in the following non-dimensional form (omitting the primes):

$$\begin{aligned} \frac{\partial u}{\partial t} &= -\Delta^2 u - \lambda\Delta u + \Delta(\gamma_2 u^2 + \gamma_3 u^3) - \sigma u, \\ \int_\Omega u(x,t)\,\mathrm{d}x &= 0, \\ \frac{\partial u}{\partial n} &= \frac{\partial \Delta u}{\partial n} = 0 \qquad \text{on } \partial\Omega, \\ u(x,0) &= \psi, \end{aligned} \tag{2.6}$$

where $\Omega = \prod_{i=1}^{3}(0, L_i)$, and $L_i = L_i^d/d, 1 \le i \le 3$. Note that since $b_3 > 0$ by our assumption, we have $\gamma_3 > 0$.

For the mathematical set-up, let us introduce the following function spaces:

$$\begin{aligned} H &:= \left\{ u \in L^2(\Omega) \,\middle|\, \int_\Omega u\,\mathrm{d}x = 0 \right\}, \\ H_1 &:= \left\{ u \in H^4(\Omega) \cap H \,\middle|\, \frac{\partial u}{\partial n} = \frac{\partial \Delta u}{\partial n} = 0 \text{ on } \partial\Omega \right\}, \\ H_{1/2} &:= \left\{ u \in H^2(\Omega) \cap H \,\middle|\, \frac{\partial u}{\partial n} = 0 \text{ on } \partial\Omega \right\}. \end{aligned} \tag{2.7}$$

We define the operators $L_\lambda = -A + B_\lambda : H_1 \to H$ and $G : H_{1/2} \to H$ by

$$\begin{aligned} Au &= \Delta^2 u, \\ B_\lambda u &= -\lambda \Delta u - \sigma u, \\ G(u) &= \gamma_2 \Delta u^2 + \gamma_3 \Delta u^3. \end{aligned} \tag{2.8}$$

Then, the system (2.6) is equivalent to the following abstract form:

$$\begin{aligned} \frac{\mathrm{d}u}{\mathrm{d}t} &= L_\lambda u + G(u), \\ u(0) &= \psi, \end{aligned} \tag{2.9}$$

where $\psi \in H$ is a given function.

The existence and uniqueness of solutions to (2.9) can be proven in a standard fashion; see, e.g., [24, Chap. III]. In particular, for any $\psi \in H$, the system (2.9) possesses a unique weak solution u which belongs to

$$C([0,T];H) \cap L^2((0,T);H_{1/2}), \quad \forall T > 0.$$

Moreover, if $\psi \in H_{1/2}$, then $u \in C([0,T];H_{1/2}) \cap L^2((0,T);H_1)$ for all $T > 0$.

3. Principle of exchange of stabilities

In this section, we consider the eigenvalue problem associated with the linear operator L_λ as defined in (2.8). For this purpose, Let us first consider the following eigenvalue problem:

$$\begin{aligned} -\Delta \psi &= \rho \psi, \\ \frac{\partial \psi}{\partial n} &= 0 \quad \text{on } \partial\Omega, \\ \int_\Omega \psi \,\mathrm{d}x &= 0. \end{aligned} \tag{3.1}$$

Since the domain Ω is rectangular, the eigenvalues and eigenfunctions for the system (3.1) are given by:

$$\begin{aligned} \rho_K &= |K|^2, \\ e_K &= \cos\Big(\frac{k_1 \pi x_1}{L_1}\Big) \cos\Big(\frac{k_2 \pi x_2}{L_2}\Big) \cos\Big(\frac{k_3 \pi x_3}{L_3}\Big), \end{aligned} \tag{3.2}$$

where the wave vector K belongs to the following permissible set $\mathcal{P}$:

$$\mathcal{P} := \left\{ \Big(\frac{k_1\pi}{L_1}, \frac{k_2\pi}{L_2}, \frac{k_3\pi}{L_3}\Big) \;\Big|\; k_i \in \mathbb{N}_0, \quad 1 \le i \le 3, \quad \sum_{i=1}^{3} k_i^2 \neq 0 \right\}, \tag{3.3}$$

with $\mathbb{N}_0$ being the set of all nonnegative integers, and

$$|K|^2 := \sum_{i=1}^{3} \frac{k_i^2 \pi^2}{L_i^2}. \tag{3.4}$$

Note that the linear operator $L_\lambda = -A + B_\lambda$ defined by (2.8) has the same eigenfunctions $\{e_K \,|\, K \in \mathcal{P}\}$ as given in (3.2); and the eigenvalue of L_λ corresponding to e_K is given by

$$\beta_K(\lambda) = -|K|^4 + \lambda |K|^2 - \sigma = |K|^2 \Big(\lambda - \frac{|K|^4 + \sigma}{|K|^2}\Big), \qquad K \in \mathcal{P}. \tag{3.5}$$

The linear stability and instability are precisely determined by the critical-crossing of the first eigenvalue, which is often called the principle of exchange of stabilities (PES). For this purpose, we define a number λ_c as follows:

$$\lambda_c := \min_{K\in\mathcal{P}} \frac{|K|^4+\sigma}{|K|^2}. \tag{3.6}$$

Note that λ_c is the critical value of the parameter λ at which some eigenvalues of L_λ cross the imaginary axis and the rest remain on the left half plane.

Let us denote by $\mathcal{S}$ the set of critical wave vectors that achieve the minimum in (3.6):

$$\mathcal{S} := \{ K\in\mathcal{P} \mid K \text{ achieves the minimum in (3.6)} \}. \tag{3.7}$$

Then, the following PES condition holds:

$$\beta_K(\lambda) \begin{cases} <0 & \text{if } \lambda<\lambda_c, \\ =0 & \text{if } \lambda=\lambda_c, \\ >0 & \text{if } \lambda>\lambda_c, \end{cases} \qquad \forall\, K\in\mathcal{S}, \tag{3.8}$$

$$\beta_K(\lambda_c)<0 \qquad \forall\, K\in\mathcal{P}\backslash\mathcal{S}. \tag{3.9}$$

The above condition implies that λ_c is exactly the critical value of λ, at which the disordered state $u\equiv 0$ of the system (2.9) loses its linear stability.

4. Dynamic transitions and pattern formations

From dynamic transition theory [14, 16] (see also appendix A), we know that as λ crosses λ_c from below, the system (2.9) always undergoes a dynamic transition of one of three types: Type-I, Type-II, and Type-III; and the type of transition is mainly dictated by the nonlinear interactions in the system. In this section, we address the type of phase transitions and the associated pattern formations. The proofs are deferred to next section.

4.1. Transitions to LAM patterns. In this subsection, we consider the case where the first eigenvalue is simple and the corresponding critical wave vector K_1 which achieves the minimum in (3.6) is of the form $K_1=(k_1\pi/L_1,\ 0,\ 0)$, for some $k_1\in\mathbb{N}$. We will see later in Section 5 that the type and structure of phase transitions of the system are dictated by the sign of the following parameter:

$$\mathcal{B} := \gamma_3 - \frac{8|K_1|^2}{36|K_1|^4-9\sigma}\gamma_2^2. \tag{4.1}$$

One can readily check by (3.6) that $|K_1|^2\simeq\sqrt{\sigma}$, the parameter $\mathcal{B}$ then takes the following simpler form:

$$\mathcal{B} \simeq \gamma_3 - \frac{8}{27}\frac{\gamma_2^2}{\sqrt{\sigma}}. \tag{4.2}$$

THEOREM 4.1. *If $K_1=(k_1\pi/L_1,\ 0,\ 0)$ for some $k_1\in\mathbb{N}$ is the only wave vector which achieves the minimum given in* (3.6)*, the following assertions hold:*

(i) If $\mathcal{B}>0$, then the transition associated with the system (2.6) at λ_c is Type-I, where $\lambda_c=(|K_1|^4+\sigma)/|K_1|^2$ and $|K_1|^2=k_1^2\pi^2/L_1^2$. Moreover, the system bifurcates on $\lambda>\lambda_c$ to two locally stable steady states u_1 and u_2, which admit the following approximation formula:

$$u_{1,2}=\pm\sqrt{\frac{4\beta_{K_1}(\lambda)}{3|K_1|^2\mathcal{B}}}\cos(\frac{k_1\pi x_1}{L_1})+o(|\beta_{K_1}(\lambda)|^{1/2}), \tag{4.3}$$

where $\beta_{K_1}(\lambda)$ is the eigenvalue corresponds to the wave vector K_1 given by (3.5).

(ii) If $\mathcal{B}<0$, then the phase transition is Type-II, and the system bifurcates on the side $\lambda<\lambda_c$ to two non-degenerate saddle points.

From the above results, we can obtain the corresponding local phase diagrams for λ near the critical value λ_c; see Figure 4.1 below. Note that they are the same as the classical phase diagrams dictated respectively by the subcritical and supercritical pitchfork bifurcation. This figure also provides a pictorial explanation of the Type-I and Type-II transitions as recalled in Theorem A.1 for the case considered here.

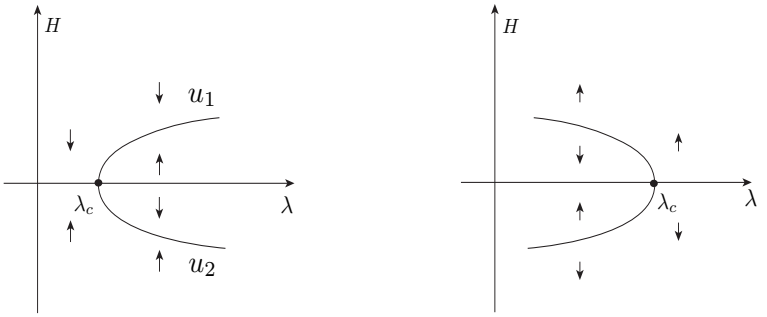

(a) $\mathcal{B}>0$ (b) $\mathcal{B}<0$

Fig. 4.1: *Phase diagram for the LAM case given in Theorem 4.1. (a) Type-I transition (when $\mathcal{B}>0$). (b) Type-II transition (when $\mathcal{B}<0$).*

For Type-I transition cases, Theorem 4.1 shows that the patterns emerging from the transition are perturbations of the pattern determined by the eigenmode e_{K_1}, which is the mode that loses its stability during the phase transition; see (4.3). Note that the spatial patterns associated with the local attractors $u_{1,2}$ given by (4.3) is laminar as illustrated in Figure 4.2.

For Type-II transition cases, although the states after the transition cannot be described precisely as is done for the Type-I transition case, it is interesting to mention that a skeleton of the corresponding global phase diagram can be obtained by using standard energy estimates; see Figure 4.3. In particular, there exists $\lambda_*<\lambda_c$ such that the disordered state $u=0$ is globally stable when $\lambda<\lambda_*$.[3] When the control parameter λ is between λ_* and λ_c, the disordered state is metastable. In this parameter regime, perturbations can lead the system to other metastable states which may be far away from the disordered one as illustrated by the top and bottom parts of the curve in Figure 4.3. The disordered state becomes unstable when $\lambda>\lambda_c$, and the phase of the

[3]which follows from standard energy estimates. See, e.g., the proof of Theorem 3.2 in [15], where the classical Cahn–Hilliard equation is dealt with (correpsonding to the case $\sigma=0$ here).

system "jumps" to these "far away" states under arbitrarily small perturbations. The two values λ_* and λ_c in Figure 4.3 represent respectively the so called *binodal* and *spinodal* points [2, 3].

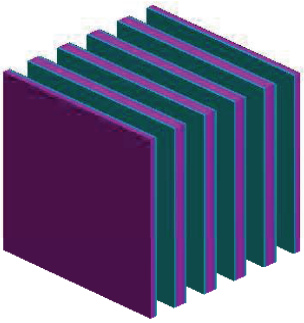

Fig. 4.2: *LAM pattern: an isosurface plot of the eigenmode* $e_{K_1}(x_1,x_2,x_3) = \cos(\frac{k_1\pi x_1}{L_1})$ *associated with the bifurcated local attractors* $u_{1,2}$ *given by* (4.3).

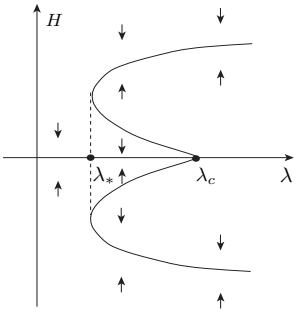

Fig. 4.3: *A global version of Figure 4.1(b): The disordered state* $u=0$ *is globally stable when* $\lambda<\lambda_*$, *is metastable when* $\lambda_*<\lambda<\lambda_c$, *and becomes unstable when* $\lambda>\lambda_c$; *see the main text for more details.*

Note also that a Type-II transition corresponds to a first-order transition in the sense of Ehrenfest, and a Type-I transition corresponds to a second-order or higher-order transition [21].

4.2. Transitions to HPC patterns. Now, we consider a transition scenario which allows hexagonally packed cylinder (HPC) patterns. We assume that the domain size satisfies the following conditions:

$$L_1 = 2\pi L,\ L_2 = \frac{2}{\sqrt{3}}\pi L,\ \text{and}\ L_3 = \theta\pi L. \tag{4.4}$$

Here, L and θ are positive constants depending on σ, which are chosen in a way such that $K_1^c := (\frac{n}{L},0,0)$ and $K_2^c := (\frac{n}{2L},\frac{\sqrt{3}n}{2L},0)$ are the only wave vectors which achieve the minimum in (3.6), where n is a positive integer.

THEOREM 4.2. *Assume that the size of the domain satisfies* (4.4), *and that* $K_1^c = (\frac{n}{L},0,0)$ *and* $K_2^c = (\frac{n}{2L},\frac{\sqrt{3}n}{2L},0)$ *are the only two wave vectors which achieve the minimum in* (3.6). *Let* $\mathcal{B}$ *be the parameter defined in* (4.1) *with* $|K_1| = |K_1^c| = |K_2^c|$. *The following assertions hold:*

(i) If

$$\gamma_2 = 0,$$

then the phase transition of (2.6) *at* λ_c *is Type-I, where* $\lambda_c = (|K_1^c|^4+\sigma)/|K_1^c|^2$. *The system bifurcates on the side* $\lambda>\lambda_c$ *to an attractor* Σ_λ, *which is homeomorphic to the one-dimensional unit sphere* S^1. Σ_λ *contains eight non-degenerate steady states, with four saddle points* v_1, v_2, v_3, *and* v_4 *and four minimal attractors* u_1, u_2, u_3, *and* u_4 *as shown in Figure* 4.4(*a*). *Moreover, the following*

approximation formulas hold:

$$\begin{aligned}
u_{1,3} &= \pm\sqrt{\frac{4\beta_1(\lambda)}{3|K_1^c|^2\gamma_3}}\cos(\frac{n}{L}x_1)+o(|\beta_1(\lambda)|^{1/2}),\\
u_{2,4} &= \pm\sqrt{\frac{16\beta_1(\lambda)}{9|K_1^c|^2\gamma_3}}\cos(\frac{n}{2L}x_1)\cos(\frac{\sqrt{3}n}{2L}x_2)+o(|\beta_1(\lambda)|^{1/2}),\\
v_{1,2,3,4} &= \pm\sqrt{\frac{4\beta_1(\lambda)}{15|K_1^c|^2\gamma_3}}\cos(\frac{n}{L}x_1)\\
&\quad \pm 2\sqrt{\frac{4\beta_1(\lambda)}{15|K_1^c|^2\gamma_3}}\cos(\frac{n}{2L}x_1)\cos(\frac{\sqrt{3}n}{2L}x_2)+o(|\beta_1(\lambda)|^{1/2}),
\end{aligned} \tag{4.5}$$

where $\beta_1(\lambda):=\beta_{K_1^c}(\lambda)$ *is as given in* (3.5).

(ii) If

$$\gamma_2\neq 0 \text{ and } \mathcal{B}<0,$$

then the system (2.6) *bifurcates on both sides of* λ_c *and the transition is Type-II. Moreover, there are four steady states bifurcated out on the side* $\lambda<\lambda_c$*, including three saddle points and one unstable node. On the side* $\lambda>\lambda_c$*, the system bifurcates to two steady states, which are saddles.*

(iii) If

$$\gamma_2\neq 0 \text{ and } \mathcal{B}>0,$$

then the transition is Type-III.
Again, there are bifurcations on both sides of λ_c*. On the side* $\lambda<\lambda_c$*, there are two saddles bifurcating out from the origin.*
On the side $\lambda>\lambda_c$*, the system bifurcates to four steady states:*

$$\begin{aligned}
w_1 &= \frac{\beta_1(\lambda)}{|K_1^c|^2\gamma_2}\cos(\frac{n}{L}x_1)+\frac{2\beta_1(\lambda)}{|K_1^c|^2\gamma_2}\cos(\frac{n}{2L}x_1)\cos(\frac{\sqrt{3}n}{2L}x_2)+o(|\beta_1(\lambda)|),\\
w_2 &= \frac{\beta_1(\lambda)}{|K_1^c|^2\gamma_2}\cos(\frac{n}{L}x_1)-\frac{2\beta_1(\lambda)}{|K_1^c|^2\gamma_2}\cos(\frac{n}{2L}x_1)\cos(\frac{\sqrt{3}n}{2L}x_2)+o(|\beta_1(\lambda)|),\\
w_3 &= \sqrt{-\frac{\beta_1(\lambda)}{b(\lambda)}}\cos(\frac{n}{L}x_1)+o(|\beta_1(\lambda)|^{1/2}),\\
w_4 &= -\sqrt{-\frac{\beta_1(\lambda)}{b(\lambda)}}\cos(\frac{n}{L}x_1)+o(|\beta_1(\lambda)|^{1/2}),
\end{aligned} \tag{4.6}$$

where $b(\lambda)=\frac{2|K_1^c|^4\gamma_2^2}{16|K_1^c|^4-4\lambda|K_1^c|^2+\sigma}-\frac{3|K_1^c|^2}{4}\gamma_3$*. Among the four steady states, there are one stable node and three saddles, where the node is* w_3 *if* $\gamma_2>0$*, and* w_4 *if* $\gamma_2<0$*.*
Moreover, there is a neighborhood $V\subset H$ *of* $u=0$*, which can be decomposed into two disjoint sectorial regions* V_I *and* V_{II} *such that* $\overline{V}=\overline{V}_I\cup\overline{V}_{II}$ *and the phase transition is Type-I if the initial perturbation is in* V_I *and is Type-II if the initial perturbation is in* V_{II}*. In region* V_I*, there is exactly one minimal attractor as is shown in Figure* 4.4(*b*) *for* $\gamma_2>0$ *and in Figure* 4.4(*c*) *for* $\gamma_2<0$*.*

We note that, among all the steady states given in (4.5), u_1 adn u_3 are related to LAM patterns as shown in Figure 4.2, v_1, v_2, v_3, and v_4 lead to HPC patterns shown in Figure 4.5, and u_2 and u_4 correspond to rectangular patterns as shown in Figure 4.6. Similarly, among the steady states given in (4.6), w_1 and w_2 correspond to HPC patterns, and w_3 and w_4 correspond to LAM patterns.

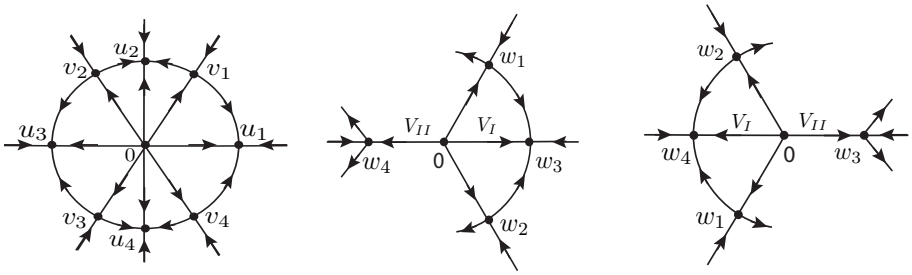

(a) $\gamma_2 = 0$ (b) $\gamma_2 > 0$ and $\mathcal{B} > 0$ (c) $\gamma_2 < 0$ and $\mathcal{B} > 0$

Fig. 4.4: *Local phase portrait for the HPC case stated in Theorem 4.2. (a) Type-I transition (when $\gamma_2 = 0$): the attractor Σ_λ after the transition is mapped homeomorphically to S^1 and u_1, u_2, u_3 and u_4 are minimal attractors. (b) Type-III transition (when $\gamma_2 > 0$ and $\mathcal{B} > 0$): the sectorial regions V_I and V_{II} are separated by the stable manifolds of the steady states w_1 and w_2 represented by the lines $\overline{0w_1}$ and $\overline{0w_2}$ respectively, and w_3 is the minimal attractor in V_I. (c) Type-III transition (when $\gamma_2 < 0$ and $\mathcal{B} > 0$): the sectorial regions V_I and V_{II} are separated again by the stable manifolds of the steady states w_1 and w_2, and w_4 is the minimal attractor in region V_I.*

In Type-I transition cases, as the disordered state loses its stability, the transition happens in two stages as time evolves: First, there is a fast transition from the disordered state towards the bifurcated attractor Σ_λ; then there is a slow evolution within the bifurcated structure. Depending on the initial perturbations, the patterns finally emerging from the transition may be either lamellae or rectangles.

In Type-III transition cases, transition may happen on both sides of the critical point λ_c. On the side $\lambda < \lambda_c$, the disordered state is metastable, and perturbations may drive the system to some other metastable states far away from the disordered state; see also the discussion at the end of the previous subsection. On the side $\lambda > \lambda_c$, the disordered state is unstable, and the transition may be either Type-I or Type-II depending on the initial perturbations. When the perturbation leads to Type-I transition, as time evolves, there is first a fast transition towards the local attractor which consists of two steady states with the HPC structure, one steady state with LAM structure, and two heteroclinic orbits connecting them as shown in figures 4.4(b) and 4.4(c); the pattern eventually settles down to LAM patterns.

4.3. Transitions to rectangle and sphere patterns. In this subsection, we return to the situation when the first eigenvalue is simple, and we study the case when the corresponding wave vector K_1 that achieves the minimum in (3.6) is of the form

$$K_1 = (k_1\pi/L_1,\ k_2\pi/L_2,\ 0), \qquad k_i \neq 0, \quad 1 \leq i \leq 2,$$

or

$$K_1 = (k_1\pi/L_1,\ k_2\pi/L_2,\ k_3\pi/L_3), \qquad k_i \neq 0, \quad 1 \leq i \leq 3.$$

For simplicity, we will give results for the case $k_1/L_1 = k_2/L_2 = k_3/L_3$; the general situation can be dealt with in the same way. With this assumption, the eigenfunction corresponding to the first eigenvalue has a square pattern when $K_1 = (k_1\pi/L_1,\ k_2\pi/L_2,\ 0)$,

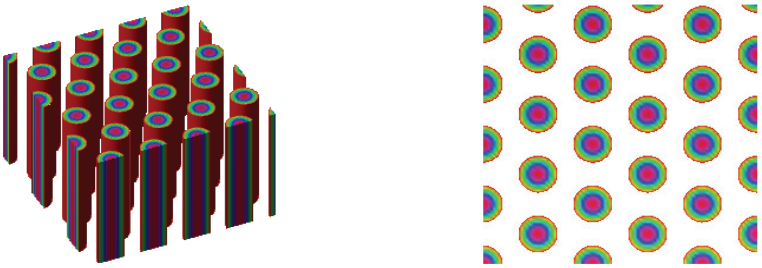

(a) (b)

Fig. 4.5: *(a) HPC structures determined by* $v_{1,2,3,4}$ *in* (4.5). *Here, the figure is obtained as an isosurface plot of the function* $\cos(\frac{nx_1}{L})+2\cos(\frac{nx_1}{2L})\cos(\frac{\sqrt{3}nx_2}{2L})$. *(b) Top view of the structures given in (a).*

and a sphere pattern when $K_1=(k_1\pi/L_1,\ k_2\pi/L_2,\ k_3\pi/L_3)$. We define the following parameters:

$$\begin{aligned}\mathcal{B}_2 &:= \gamma_3 - \frac{16}{9}\left(\frac{|K_1|^2}{2|K_1|^4-\sigma}+\frac{|K_1|^2}{2\big(12|K_1|^4-3\sigma\big)}\right)\gamma_2^2,\\ \mathcal{B}_3 &:= \gamma_3 - \frac{32|K_1|^2}{3}\left(\frac{1}{4|K_1|^4-3\sigma}+\frac{1}{40|K_1|^4-15\sigma}+\frac{1}{108(4|K_1|^4-\sigma)}\right)\gamma_2^2.\end{aligned} \tag{4.7}$$

THEOREM 4.3. *Assume that* $K_1=(k_1\pi/L_1,\ k_2\pi/L_2,\ 0)$, $k_1/L_1=k_2/L_2\neq 0$, *is the only wave vector which satisfies* (3.6). *Then the following assertions hold:*

(i) If

$$\mathcal{B}_2<0,$$

then the phase transition of (2.6) *at* λ_c *is Type-II. In particular, the system bifurcates from* $(u,\lambda)=(0,\lambda_c)$ *on the side* $\lambda<\lambda_c$ *to two non-degenerate saddle points.*

(ii) If

$$\mathcal{B}_2>0,$$

the transition is Type-I, and the system bifurcates on $\lambda>\lambda_c$ *to two local attractors* u_1 *and* u_2, *which can be expressed as*

$$u_{1,2}=\pm\sqrt{\frac{16\beta_{K_1}(\lambda)}{9|K_1|^2\mathcal{B}_2}}\cos(\frac{k_1\pi x_1}{L_1})\cos(\frac{k_2\pi x_2}{L_2})+o(|\beta_{K_1}(\lambda)|^{1/2}), \tag{4.8}$$

where $\beta_{K_1}(\lambda)$ *is as in* (3.5).

See Figure 4.6 for a plot of the spatial structure of $u_{1,2}$ given in Theorem 4.3.

THEOREM 4.4. *Assume that the only wave vector which satisfies* (3.6) *is* $K_1=(k_1\pi/L_1,\ k_2\pi/L_2,\ k_3\pi/L_3)$, $k_1/L_1=k_2/L_2=k_3/L_3\neq 0$. *Then the following assertions hold:*

(i) If

$$\mathcal{B}_3<0,$$

then the phase transition of (2.6) *at* λ_c *is Type-II. In particular, the system bifurcates on the side* $\lambda<\lambda_c$ *to two non-degenerate saddle points.*

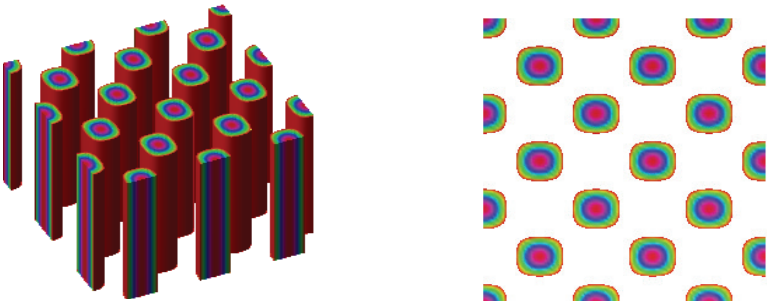

(a) (b)

Fig. 4.6: *(a) Rectangle patterns: an isosurface plot of the eigenmode* $\cos(\frac{k_1\pi x_1}{L_1})\cos(\frac{k_2\pi x_2}{L_2})$ *associated with the local attractor given by* (4.8). *(b) Top view of the structures given in (a).*

(ii) If

$$\mathcal{B}_3 > 0,$$

the transition is Type-I, and the system bifurcates on $\lambda > \lambda_c$ *to two attractors* u_1 *and* u_2*, which can be expressed as*

$$u_{1,2} = \pm\sqrt{\frac{64\beta_{K_1}(\lambda)}{27|K_1|^2\mathcal{B}_3}}\cos(\frac{k_1\pi x_1}{L_1})\cos(\frac{k_2\pi x_2}{L_2})\cos(\frac{k_3\pi x_3}{L_3}) + o(|\beta_{K_1}(\lambda)|^{1/2}), \tag{4.9}$$

where $\beta_{K_1}(\lambda)$ *is as in* (3.5).

See Figure 4.7 for a plot of the spatial structure of $u_{1,2}$ given in Theorem 4.4.

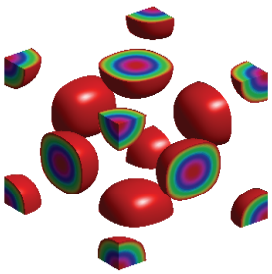

Fig. 4.7: *Sphere patterns in face-centered-cubic lattices: an isosurface plot of the eigenmode* $\cos(\frac{k_1\pi x_1}{L_1})\cos(\frac{k_2\pi x_2}{L_2})\cos(\frac{k_3\pi x_3}{L_3})$ *associated with the local attractor given by* (4.9).

5. Proofs of the main theorems

This section is devoted to the proofs of the main results regarding the phase transitions associated with the system (2.6) presented in the previous section.

Proof. (**Proof of Theorem 4.1.**) The proof relies on the center manifold reduction, which reduces the system (2.6) to a one-dimensional ODE for the case considered here. We follow the treatment presented in [14, 16]; see also Appendix A for a brief account of this theory.

For this purpose, let us first introduce the subspaces H_c and H_s by

$$H_c := \text{span}\{e_{K_1}\}, \qquad H = H_c \oplus H_s, \tag{5.1}$$

namely, H_c is the center-subspace spanned by the eigenmode which loses its stability as λ crosses the critical value λ_c, and H_s is the stable-subspace obtained as the topological complement of H_c in the ambient space H, where H is defined in (2.7). Let us also denote by P_c and P_s the corresponding canonical projectors associated with H_c and H_s respectively.

Note that any solution $u(t,x,\lambda)$ of the system (2.6) on the center manifold takes the following form:

$$u(t,x,\lambda) = y(t,\lambda)e_{K_1}(x) + \Phi(y(t,\lambda)e_{K_1}(x),\lambda), \tag{5.2}$$

where $y(t,\lambda)e_{K_1}(x) = P_c u(t,x,\lambda)$, and $\Phi(\cdot,\lambda): H_c \to H_s$ is the center manifold function which we will calculate later.[4] Recall that thanks to the classical center manifold theorem [11, 14, 24], we have

$$\Phi(y(t,\lambda)e_{K_1},\lambda) = o(|y(t,\lambda)|). \tag{5.3}$$

Now multiplying both sides of the first equation in the system (2.6) by e_{K_1} and integrating over Ω, we obtain the following equation for $y(t,\lambda)$:

$$\frac{\mathrm{d}y}{\mathrm{d}t} = \beta_{K_1}(\lambda)y - \frac{1}{\langle e_{K_1}, e_{K_1}\rangle}\int_\Omega \Delta(\gamma_2 u^2 + \gamma_3 u^3)e_{K_1}\,\mathrm{d}x,$$

where $\langle\cdot,\cdot\rangle$ stands for the inner product in H.

Applying integration by parts twice in the above equality and using the identity $\Delta e_{K_1} = -|K_1|^2 e_{K_1}$, we get then

$$\frac{\mathrm{d}y}{\mathrm{d}t} = \beta_{K_1}(\lambda)y - \frac{2|K_1|^2}{|\Omega|}\int_\Omega (\gamma_2 u^2 + \gamma_3 u^3)e_{K_1}\,\mathrm{d}x,$$

where $|\Omega|$ is the volume of Ω.

Now, by using the representation of solution on the center manifold given by (5.2) and the fact that $\Phi(y(t,\lambda)e_{K_1},\lambda) = o(|y(t,\lambda)|)$ recalled in (5.3), we derive the following reduced equation on the center manifold:

$$\frac{\mathrm{d}y}{\mathrm{d}t} = \beta_{K_1}(\lambda)y - \frac{2|K_1|^2}{|\Omega|}\big(g_2(y) + g_3(y) + g_{23}(y)\big) + o(|y|^3), \tag{5.4}$$

where

$$g_2(y) = \gamma_2 y^2 \int_\Omega e_{K_1}^2 e_{K_1}\,\mathrm{d}x, \tag{5.5}$$

$$g_3(y) = \gamma_3 y^3 \int_\Omega e_{K_1}^3 e_{K_1}\,\mathrm{d}x, \tag{5.6}$$

$$g_{23}(y) = 2\gamma_2 y \int_\Omega e_{K_1}\Phi(y e_{K_1},\lambda)e_{K_1}\,\mathrm{d}x. \tag{5.7}$$

By using basic trigonometric identities, we obtain

$$g_2(y) = \gamma_2 y^2 \int_\Omega \cos^3(k_1\pi x_1/L_1)\,\mathrm{d}x = 0, \tag{5.8}$$

[4] Note that the center manifold function Φ actually takes values in a more regular space $H^s_{1/2}$, where $H^s_{1/2}$ is the topological complement of H_c in the space $H_{1/2}$ with the latter defined in (2.7). However, we will not make use of this regularity in this proof.

$$g_3(y)=\gamma_3 y^3\int_\Omega \cos^4(k_1\pi x_1/L_1)\,\mathrm{d}x=\frac{3\gamma_3}{8}|\Omega|y^3. \tag{5.9}$$

To evaluate g_{23}, we need to compute the center manifold function $\Phi(ye_{K_1},\lambda)$. We will use the following second order approximation formula of $\Phi(ye_{K_1},\lambda)$ (see, e.g., [14, Thm. 3.8] for details; see also Appendix A):

$$\Phi(ye_{K_1},\lambda)=(-L_\lambda^s)^{-1}P_sG_2(ye_{K_1})+o(2). \tag{5.10}$$

Here $P_s: H\to H_s$ is the canonical projection with H_s being the subspace of H spanned by all stable eigenfunctions of L_λ as defined by (5.1), L_λ^s is the restriction of L_λ to H_s, G_2 is the second order term of the nonlinearity, i.e., $G_2(v)=\gamma_2\Delta v^2$, and the $o(2)$-term is given by

$$o(k):=O(|\beta_{K_1}(\lambda)||y|^k)+o(|y|^k),\qquad k\in\mathbb{N}. \tag{5.11}$$

Since $\{e_K\,|\,K\in\mathcal{P}\setminus K_1\}$ spans H_s, we can write Φ in the following form:

$$\Phi(ye_{K_1},\lambda)=\sum_{K\in\mathcal{P}\setminus\{(k_1\pi/L_1,0,0)\}}\frac{\langle\Phi(ye_{K_1},\lambda),e_K\rangle}{\langle e_K,e_K\rangle}e_K. \tag{5.12}$$

Now, for each e_K with $K\in\mathcal{P}\setminus\{(k_1\pi/L_1,0,0)\}$, we take the L^2 inner product of (5.10) with e_K to obtain

$$\begin{aligned}\langle\Phi(ye_{K_1},\lambda),e_K\rangle&=\langle(-L_\lambda^s)^{-1}P_sG_2(ye_{K_1}),e_K\rangle+o(2)\\&=\langle P_sG_2(ye_{K_1}),(-L_\lambda^s)^{-1}e_K\rangle+o(2)\\&=-\frac{1}{\beta_K(\lambda)}\langle G_2(ye_{K_1}),e_K\rangle+o(2),\qquad\forall K\in\mathcal{P}\setminus\{(k_1\pi/L_1,0,0)\}.\end{aligned}$$

Using this identity in (5.12), we obtain

$$\Phi(ye_{K_1},\lambda)=\sum_{K\in\mathcal{P}\setminus\{(k_1\pi/L_1,0,0)\}}-\frac{\langle G_2(ye_{K_1}),e_K\rangle}{\beta_K(\lambda)\langle e_K,e_K\rangle}e_K+o(2). \tag{5.13}$$

Recall also that $G_2(v)=\gamma_2\Delta v^2$, which leads to

$$\frac{\langle G_2(ye_{K_1}),e_K\rangle}{\beta_K(\lambda)\langle e_K,e_K\rangle}=\frac{\gamma_2y^2\langle e_{K_1}^2,\Delta e_K\rangle}{\beta_K(\lambda)\langle e_K,e_K\rangle}=-\frac{\gamma_2|K|^2y^2}{\beta_K(\lambda)\langle e_K,e_K\rangle}\int_\Omega e_{K_1}^2e_K\,\mathrm{d}x.$$

Note that

$$\int_\Omega e_{K_1}^2e_K\,\mathrm{d}x=\int_\Omega\frac{1+\cos(2k_1\pi x_1/L_1)}{2}e_K\,\mathrm{d}x=\begin{cases}|\Omega|/4, & \text{if } K=(2k_1\pi/L_1,0,0),\\ 0, & \text{otherwise.}\end{cases}$$

It follows then that the center manifold function $\Phi(ye_{K_1},\lambda)$ can be approximated via:

$$\Phi(ye_{K_1},\lambda)=\frac{2\gamma_2|K_1|^2y^2}{\beta_{2K_1}(\lambda)}\cos(\frac{2k_1\pi x_1}{L_1})+o(2). \tag{5.14}$$

By using (5.14) in (5.7), we get

$$g_{23}(y)=\frac{\gamma_2^2|K_1|^2|\Omega|}{\beta_{2K_1}(\lambda)}y^3+o(3). \tag{5.15}$$

Finally, by reporting (5.8), (5.9) and (5.15) in (5.4), we derive after simplification the following reduced equation for the system (2.6):

$$\frac{\mathrm{d}y}{\mathrm{d}t}=\beta_{K_1}(\lambda)y-2|K_1|^2\Big(\frac{3}{8}\gamma_3+\frac{|K_1|^2}{\beta_{2K_1}(\lambda)}\gamma_2^2\Big)y^3+o(3). \tag{5.16}$$

Thanks to the classical center manifold theory, the transition of the system (2.6) in this case is the same as the transition of the reduced system (5.16); see, e.g., [14, Chap. 6] and [16, Chap. 2].

Note that (5.16) has a pitchfork bifurcation at $(y,\lambda)=(0,\lambda_c)$, and the sign of the cubic term determines whether the bifurcation at λ_c is supercritical or subcritical. For this purpose, we introduce a parameter $\mathcal{B}$ as follows:

$$\mathcal{B}:=\gamma_3+\frac{8|K_1|^2}{3\beta_{2K_1}(\lambda_c)}\gamma_2^2=\gamma_3-\frac{8|K_1|^2}{36|K_1|^4-9\sigma}\gamma_2^2. \tag{5.17}$$

If $\mathcal{B}>0$, then the bifurcation at λ_c is supercritical, i.e., the bifurcation occurs on the side $\lambda>\lambda_c$, and the two bifurcated steady states are local attractors, which can be expressed as

$$y_{1,2}(\lambda)=\pm\sqrt{\frac{4\beta_{K_1}(\lambda)}{3|K_1|^2\mathcal{B}}}+o(\sqrt{\beta_{K_1}(\lambda)}).$$

Since all initial data in a sufficiently small neighborhood of the trivial steady state is attracted by either $y_1(\lambda)$ or $y_2(\lambda)$, and $\lim_{\lambda\to\lambda_c}|y_{1,2}(\lambda)|=0$, the transition for the reduced Equation (5.16) in this case is Type-I; see Theorem A.1. Consequently, the system (2.6) also undergoes a Type-I transition at $(u,\lambda)=(0,\lambda_c)$. Moreover, the two bifurcated attractors for system (2.6) in correspondence to $y_{1,2}(\lambda)$ take the form given by (4.3). Assertion (i) is now proved.

If $\mathcal{B}<0$, then the bifurcation at λ_c is subcritical, i.e., the bifurcation occurs on the side $\lambda<\lambda_c$, and the two bifurcated steady states are non-degenerate saddle points. On the side $\lambda>\lambda_c$, it can be checked that the direction of the vector field on the RHS of (5.16) points away from the origin in a neighborhood of the trivial steady state, where the size of the neighborhood can be chosen to be independent of λ. The transition for this case is thus Type-II; see Theorem A.1. Hence, Assertion (ii) is justified. The proof is now complete. ∎

Proof. **(Proof of Theorem 4.2.)** We proceed in three steps.

Step 1. Derivation of the reduced system. The eigenfunctions of L_λ corresponding to K_1^c and K_2^c are

$$e_1(x)=\cos(\frac{n}{L}x_1),\qquad e_2(x)=\cos(\frac{n}{2L}x_1)\cos(\frac{\sqrt{3}n}{2L}x_2). \tag{5.18}$$

In this case, the center-subspace H_c is spanned by the two eigenmodes e_1 and e_2:

$$H_c:=\mathrm{span}\{e_1,e_2\}. \tag{5.19}$$

As before, let us write any given solution $u(t,x,\lambda)$ of the system (2.6) on the center manifold as

$$u(t,x,\lambda)=v(t,x,\lambda)+\Phi(v(t,x,\lambda),\lambda),$$

where $v(t,x,\lambda)=P_c u(t,x,\lambda)=y_1(t,\lambda)e_1(x)+y_2(t,\lambda)e_2(x)$ and $\Phi(\cdot,\lambda):H_c\to H_s$ is the center manifold function. Again, Φ can be approximated to the second order via the formula recalled in (A.8), namely

$$\Phi(y_1e_1+y_2e_2,\lambda)=(-L_\lambda^s)^{-1}P_sG_2(y_1e_1+y_2e_2)+o(2), \tag{5.20}$$

where $o(2)$ is defined in (5.11), with (y_1,y_2) in place of y therein.

Following the same reasoning as in (5.12)–(5.14), we can derive the following:

$$\begin{aligned}\Phi(y_1e_1+y_2e_2,\lambda)=&-\frac{2\gamma_2|K_1^c|^2y_1^2}{16|K_1^c|^4-4\lambda|K_1^c|^2+\sigma}\cos(\frac{2n}{L}x_1)\\&-\frac{3\gamma_2|K_1^c|^2y_1y_2}{9|K_1^c|^4-3\lambda|K_1^c|^2+\sigma}\cos(\frac{3n}{2L}x_1)\cos(\frac{\sqrt{3}n}{2L}x_2)\\&-\frac{\gamma_2|K_1^c|^2y_2^2}{16|K_1^c|^4-4\lambda|K_1^c|^2+\sigma}\cos(\frac{n}{L}x_1)\cos(\frac{\sqrt{3}n}{L}x_2)\\&-\frac{3\gamma_2|K_1^c|^2y_2^2}{4(9|K_1^c|^4-3\lambda|K_1^c|^2+\sigma)}\cos(\frac{\sqrt{3}n}{L}x_2)+o(2),\end{aligned} \tag{5.21}$$

where $|K_1^c|=|K_2^c|=n/L$.

Now multiplying both sides of the first equation in (2.6) by e_1 (and e_2 in turn), integrating over Ω, and making use of the approximation (5.21), we obtain the following reduced equations to the center manifold:

$$\begin{aligned}\frac{\mathrm{d}y_1}{\mathrm{d}t}&=\beta_1(\lambda)y_1-\frac{|K_1^c|^2\gamma_2}{4}y_2^2+b(\lambda)y_1^3+c(\lambda)y_1y_2^2+o(3),\\\frac{\mathrm{d}y_2}{\mathrm{d}t}&=\beta_1(\lambda)y_2-|K_1^c|^2\gamma_2y_1y_2+d(\lambda)y_2^3+e(\lambda)y_1^2y_2+o(3),\end{aligned} \tag{5.22}$$

where $\beta_1(\lambda)=\beta_{K_1^c}(\lambda)=\beta_{K_2^c}(\lambda)$ and

$$\begin{aligned}b(\lambda)&=\frac{2|K_1^c|^4\gamma_2^2}{16|K_1^c|^4-4\lambda|K_1^c|^2+\sigma}-\frac{3|K_1^c|^2}{4}\gamma_3,\\c(\lambda)&=\frac{3|K_1^c|^4\gamma_2^2}{2(9|K_1^c|^4-3\lambda|K_1^c|^2+\sigma)}-\frac{3|K_1^c|^2}{4}\gamma_3,\\d(\lambda)&=\frac{|K_1^c|^4\gamma_2^2}{2(16|K_1^c|^4-4\lambda|K_1^c|^2+\sigma)}+\frac{3|K_1^c|^4\gamma_2^2}{4(9|K_1^c|^4-3\lambda|K_1^c|^2+\sigma)}-\frac{9|K_1^c|^2}{16}\gamma_3,\\e(\lambda)&=\frac{3|K_1^c|^4\gamma_2^2}{9|K_1^c|^4-3\lambda|K_1^c|^2+\sigma}-\frac{3|K_1^c|^2}{2}\gamma_3.\end{aligned} \tag{5.23}$$

Again, due to the classical center manifold theory, the transition of the system (2.6) in this case is the same as the transition of the reduced system (5.22). To analyze the latter, it is important to understand the dynamics of the reduced system at the critical parameter λ_c. At $\lambda=\lambda_c$, $\beta_1(\lambda)=0$, and (5.22) reads (up to 3rd order terms):

$$\begin{aligned}\frac{\mathrm{d}y_1}{\mathrm{d}t}&=-\frac{|K_1^c|^2\gamma_2}{4}y_2^2+b(\lambda_c)y_1^3+c(\lambda_c)y_1y_2^2,\\\frac{\mathrm{d}y_2}{\mathrm{d}t}&=-|K_1^c|^2\gamma_2y_1y_2+d(\lambda_c)y_2^3+e(\lambda_c)y_1^2y_2.\end{aligned} \tag{5.24}$$

We analyze below the cases $\gamma_2=0$ and $\gamma_2\neq0$ separately.

Step 2. The case when $\gamma_2 = 0$. In this case, (5.24) reads as

$$\begin{aligned}\frac{\mathrm{d}y_1}{\mathrm{d}t} &= -\frac{3|K_1^c|^2}{4}\gamma_3 y_1^3 - \frac{3|K_1^c|^2}{4}\gamma_3 y_1 y_2^2,\\ \frac{\mathrm{d}y_2}{\mathrm{d}t} &= -\frac{9|K_1^c|^2}{16}\gamma_3 y_2^3 - \frac{3|K_1^c|^2}{2}\gamma_3 y_1^2 y_2.\end{aligned} \tag{5.25}$$

Note that

$$\frac{\mathrm{d}(y_1^2+y_2^2)}{\mathrm{d}t} = -\frac{3|K_1^c|^2}{2}y_1^4 - \frac{9|K_1^c|^2}{8}\gamma_3 y_2^4 - 3|K_1^c|^2\gamma_3 y_1^2 y_2^2 < 0, \quad \forall (y_1,y_2)\neq(0,0).$$

Hence, the trivial steady state of (5.25) is locally asymptotically stable. Therefore, due to Theorem 6.1 in [14] (see also [15, Thm. A.3]), the transition of (5.22) is Type-I.

To determine the structure of the attractor after the transition, we can ignore the $o(3)$ terms in (5.22), and analyze the following truncated version:

$$\begin{aligned}\frac{\mathrm{d}y_1}{\mathrm{d}t} &= \beta_1(\lambda)y_1 - \frac{3|K_1^c|^2}{4}\gamma_3 y_1^3 - \frac{3|K_1^c|^2}{4}\gamma_3 y_1 y_2^2,\\ \frac{\mathrm{d}y_2}{\mathrm{d}t} &= \beta_1(\lambda)y_2 - \frac{9|K_1^c|^2}{16}\gamma_3 y_2^3 - \frac{3|K_1^c|^2}{2}\gamma_3 y_1^2 y_2.\end{aligned} \tag{5.26}$$

When $\lambda > \lambda_c$ the trivial steady state becomes unstable, and there are eight steady states bifurcating out from the origin for the above system (5.26). By direct computation, we obtain the bifurcated steady states as follows

$$\begin{aligned}X_{1,3} &= \left(\pm\sqrt{\frac{4\beta_1(\lambda)}{3|K_1^c|^2\gamma_3}},\ 0\right), \quad X_{2,4} = \left(0,\ \pm\sqrt{\frac{16\beta_1(\lambda)}{9|K_1^c|^2\gamma_3}}\right),\\ Y_{1,2,3,4} &= \left(\pm\sqrt{\frac{4\beta_1(\lambda)}{15|K_1^c|^2\gamma_3}},\ \pm 2\sqrt{\frac{4\beta_1(\lambda)}{15|K_1^c|^2\gamma_3}}\right).\end{aligned} \tag{5.27}$$

One can check, by calculating the Jacobian at the corresponding steady states, that all these steady states are non-degenerate, and $X_{1,2,3,4}$ are stable nodes and $Y_{1,2,3,4}$ are saddle points; see Figure 5.1 for the bifurcated structure.

By the center manifold reduction, the bifurcated steady states for the original system (2.6) are in one-to-one correspondence with the non-degenerated steady states given in (5.27). Hence, there are eight steady states bifurcating out for system (2.6) when λ crosses λ_c from below, and these steady states, denoted by $u_{1,3}$, $u_{2,4}$, $v_{1,2,3,4}$ (corresponding to $X_{1,3}$, $X_{2,4}$, and $Y_{1,2,3,4}$, respectively), take the form as given in (4.5). Since (2.6) is a gradient system, the bifurcated local attractor Σ_λ consists of these eight steady states together with the heteroclinic orbits connecting them (see, e.g., [5, Thm. 2.43]). Hence, Σ_λ is homeomorphic to the one-dimensional unit sphere S^1. Assertion (i) is now proven.

Step 3. Analysis of the reduced system for $\gamma_2 \neq 0$ case. Now, we consider the case when $\gamma_2 \neq 0$. The flow structure of (5.24) near the origin for this case can be analyzed using a classical theorem due to A. A. Andronov et al. [1, Chap. IX], which provides qualitative information about the local phase portrait near the origin for two-dimensional ODE systems. For the reader's convenience, the result is recalled in Theorem A.3 in the Appendix.

In order to apply this theorem to the system (5.24), we first note that since $\gamma_2 \neq 0$, the lowest order homogeneous polynomials P_m and Q_m in Theorem A.3 are given here

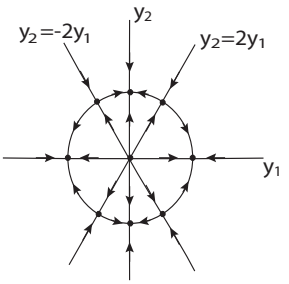

Fig. 5.1: *The local topological structure of flows of* (5.26) *when* $\beta_1(\lambda)>0$.

by the quadratic terms: $P_2(y_1,y_2):=-\frac{|K_1^c|^2\gamma_2}{4}y_2^2$ and $Q_2(y_1,y_2):=-|K_1^c|^2\gamma_2 y_1y_2$. Note also that $y_1Q_2(y_1,y_2)-y_2P_2(y_1,y_2)\not\equiv 0$, hence by Theorem A.3, any direction θ^* — along which a semipath of (5.24) tends to $O:=(0,0)$ — satisfies the equation

$$\cos\theta^* Q_2(\cos\theta^*,\sin\theta^*)-\sin\theta^* P_2(\cos\theta^*,\sin\theta^*)=0.$$

Namely,

$$-\frac{|K_1^c|^2\gamma_2}{4}(\sin^2\theta^*-4\cos^2\theta^*)\sin\theta^*=0.$$

So

$$\mod(\theta^*,2\pi)=0,\quad \pi,\quad \text{or}\quad \arctan(\pm 2), \tag{5.28}$$

where $\mod(\cdot,\cdot)$ is the standard modulo operation.

Note that the directions determined by (5.28) coincide with the directions determined by the following straight lines:

$$y_2=\pm 2y_1,\quad \text{and}\quad y_2=0. \tag{5.29}$$

We can also easily check that these three lines consist of straight line orbits of (5.24) (in the sense that trajectories starting on these lines stay on it for all $t\in\mathbb{R}$). For example, to check that $y_2=2y_1$ consists of straight line orbits, we only need to show that for any point $(y_1,2y_1)\neq(0,0)$ on this line, the ratio of the right hand sides of (5.24) is $1/2$, which can be derived as follows:

$$\begin{aligned}\frac{-\frac{|K_1^c|^2\gamma_2}{4}y_2^2+b(\lambda_c)y_1^3+c(\lambda_c)y_1y_2^2}{-|K_1^c|^2\gamma_2y_1y_2+d(\lambda_c)y_2^3+e(\lambda_c)y_1^2y_2}&=\frac{-|K_1^c|^2\gamma_2y_1^2+b(\lambda_c)y_1^3+4c(\lambda_c)y_1^3}{2\big(-|K_1^c|^2\gamma_2y_1^2+4d(\lambda_c)y_1^3+e(\lambda_c)y_1^3\big)}\\&=\frac{1}{2},\end{aligned}$$

where we have used

$$b(\lambda)+4c(\lambda)=4d(\lambda)+e(\lambda), \tag{5.30}$$

which can be derived from (5.23).

Now, the local phase portrait of (5.24) near the origin can be determined thanks to Theorem A.3. The straight line orbits serve as the separatrices, which divide the phase plane into six regions. The flow in each such region is determined by the direction of

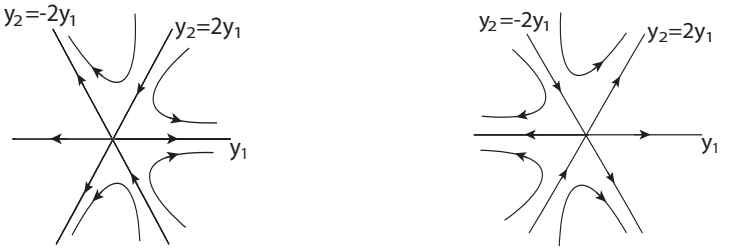

(a) $\gamma_2 > 0$ and $b(\lambda_c) > 0$ (b) $\gamma_2 < 0$ and $b(\lambda_c) > 0$

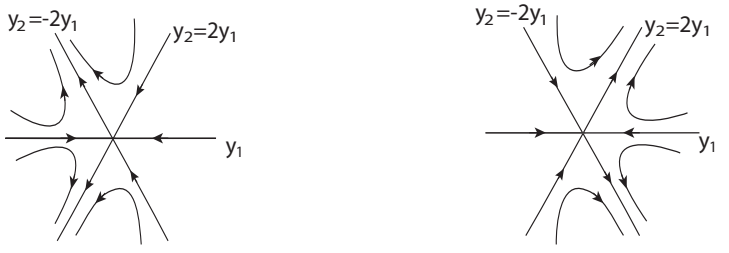

(c) $\gamma_2 > 0$ and $b(\lambda_c) < 0$ (d) $\gamma_2 < 0$ and $b(\lambda_c) < 0$

Fig. 5.2: *Topological structure of the flow of* (5.24) *near the origin when* $\gamma_2 \neq 0$.

the corresponding straight line orbits. The results depend on the signs of γ_2 and $b(\lambda_c)$, and are shown in figures 5.2(a)–5.2(d).

Based on the phase portrait of (5.24), we are in position to analyze the phase transition associated with (5.22), and we treat the two cases $b(\lambda_c) > 0$ and $b(\lambda_c) < 0$ separately.

Case $\gamma_2 \neq 0$ and $b(\lambda_c) > 0$. For $\gamma_2 \neq 0$ and $b(\lambda_c) > 0$, a neighborhood of the origin is divided into six regions by the straight line orbits of (5.24), and four of them are hyperbolic and the other two regions are parabolic as shown in figures 5.2(a) and 5.2(b). Since orbits starting from any of these regions are eventually repelled away from the origin, the transition of (5.22) is Type-II; see Theorem A.1.

Again, in order to calculate the bifurcated steady states, we can ignore the $o(3)$ terms in (5.22), and analyze the following instead

$$\beta_1(\lambda) y_1 - \frac{|K_1^c|^2 \gamma_2}{4} y_2^2 + b(\lambda) y_1^3 + c(\lambda) y_1 y_2^2 = 0, \tag{5.31a}$$

$$\beta_1(\lambda) y_2 - |K_1^c|^2 \gamma_2 y_1 y_2 + d(\lambda) y_2^3 + e(\lambda) y_1^2 y_2 = 0. \tag{5.31b}$$

In the above algebraic equations, if $y_2 = 0$, then we have from (5.31a) that

$$y_1 = \begin{cases} \pm\sqrt{-\frac{\beta_1(\lambda)}{b(\lambda)}} \text{ or } 0, & \text{if } \lambda < \lambda_c, \\ 0, & \text{if } \lambda > \lambda_c. \end{cases}$$

If $y_2 \neq 0$, we find from (5.31b) that

$$\beta_1(\lambda) = |K_1^c|^2 \gamma_2 y_1 - d(\lambda) y_2^2 + o(|y_1|). \tag{5.32}$$

By using this identity in (5.31a), we obtain

$$|K_1^c|^2 \gamma_2 y_1^2 - \left(\frac{|K_1^c|^2 \gamma_2}{4} + O(|y_1|) \right) y_2^2 + o(y_1^2) = 0, \tag{5.33}$$

which implies that $y_2 = O(|y_1|)$. By using this relation in (5.32) we obtain

$$y_1 = \frac{\beta_1(\lambda)}{|K_1^c|^2\gamma_2} + o(|\beta_1(\lambda)|). \tag{5.34}$$

This together with (5.33) leads to

$$y_2 = \pm\frac{2\beta_1(\lambda)}{|K_1^c|^2\gamma_2} + o(|\beta_1(\lambda)|).$$

From above, we conclude that for (5.22) there are four steady states bifurcating out from the origin on the side $\lambda < \lambda_c$, which are given by:

$$\begin{aligned} Z_1 &= \left(\frac{\beta_1(\lambda)}{|K_1^c|^2\gamma_2}, \frac{2\beta_1(\lambda)}{|K_1^c|^2\gamma_2}\right) + o(\beta_1(\lambda)), \quad Z_2 = \left(\frac{\beta_1(\lambda)}{|K_1^c|^2\gamma_2}, -\frac{2\beta_1(\lambda)}{|K_1^c|^2\gamma_2}\right) + o(\beta_1(\lambda)), \\ Z_3 &= \left(\sqrt{-\frac{\beta_1(\lambda)}{b(\lambda)}}, 0\right) + o(\sqrt{|\beta_1(\lambda)|}), \qquad Z_4 = \left(-\sqrt{-\frac{\beta_1(\lambda)}{b(\lambda)}}, 0\right) + o(\sqrt{|\beta_1(\lambda)|}). \end{aligned} \tag{5.35}$$

By computing the Jacobian, we can see that when λ is sufficiently close to λ_c three of them are saddle points, and the other one is an unstable node.

There are two steady states bifurcating out from the origin on the side $\lambda > \lambda_c$, which have the following form:

$$Z_5 = \left(\frac{\beta_1(\lambda)}{|K_1^c|^2\gamma_2}, \frac{2\beta_1(\lambda)}{|K_1^c|^2\gamma_2}\right) + o(\beta_1(\lambda)), \quad Z_5 = \left(\frac{\beta_1(\lambda)}{|K_1^c|^2\gamma_2}, -\frac{2\beta_1(\lambda)}{|K_1^c|^2\gamma_2}\right) + o(\beta_1(\lambda)), \tag{5.36}$$

and both of them are saddle points.

Note also that $b(\lambda_c) > 0$ is equivalent to $\mathcal{B} < 0$ with $\mathcal{B}$ given by (4.1). Assertion (ii) is thus proved.

Case $\gamma_2 \neq 0$ and $b(\lambda_c) < 0$. For $\gamma_2 \neq 0$ and $b(\lambda_c) < 0$, a neighborhood of the origin is also divided into six regions by the straight line orbits of (5.24), and four of them are hyperbolic and the other two regions are parabolic as shown in figures 5.2(c) and 5.2(d). Moreover, orbits starting in the parabolic regions tend to the origin, and orbits starting in the hyperbolic regions eventually move away from the origin. Hence, the transition of (5.22) is Type-III.

By the same type of argument used for Type-II, one can show that there are bifurcations on both sides of λ_c. On the side $\lambda < \lambda_c$, it bifurcates to two saddle points, which take the same form as in (5.36). On the side $\lambda > \lambda_c$, there are four steady states bifurcating out, which take the same form as in (5.35). When λ is sufficiently close to λ_c, one can check that three of them are non-degenerate saddle points and the other is a stable node (the stable node is Z_3 when $\gamma_2 > 0$ and is Z_4 when $\gamma_2 < 0$).

The flow structure of the reduced Equation (5.22) when $\lambda > \lambda_c$ can now be obtained easily and the result after dropping $o(|y|^3)$ terms for this case is shown in Figure 5.3. In particular, there is a neighborhood $\mathcal{N}$ of the origin of the y_1y_2 plane, which can be decomposed into two disjoint regions $\mathcal{N}_I$ and $\mathcal{N}_{II}$ such that $\overline{\mathcal{N}} = \overline{\mathcal{N}_I} \cup \overline{\mathcal{N}_{II}}$ and in region $\mathcal{N}_I$, there is exactly one stable node bifurcating out on the side $\lambda > \lambda_c$. Note that, because of the perturbations from the $o(3)$ terms, $\mathcal{N}_I$ and $\mathcal{N}_{II}$ are actually slight perturbations of the regions $\mathcal{O}_I$ and $\mathcal{O}_{II}$ in Figure 5.3, respectively. Corresponding to $\mathcal{N}$, there is a neighborhood V of the origin in space H, which can be decomposed into

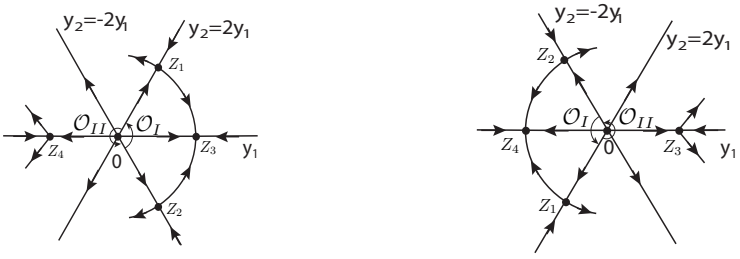

(a) $b(\lambda_c)<0$ and $\gamma_2>0$ (b) $b(\lambda_c)<0$ and $\gamma_2<0$

Fig. 5.3: *The local topological structure of flows of* (5.22) *for* $\lambda>\lambda_c$ *with* $\gamma_2\neq 0$ *and* $b(\lambda_c)<0$ *(without taking into account the* $o(3)$ *terms). The two sectorial regions* $\mathcal{O}_I$ *and* $\mathcal{O}_{II}$ *are separated by the rays* $\overline{0Z_1}$ *and* $\overline{0Z_2}$.

two disjoint regions V_I and V_{II} such that $\overline{V}=\overline{V}_I\cup\overline{V}_{II}$. Here V_I and V_{II} are chosen such that

$$P_cV_I=\mathcal{N}_I,\quad P_cV_{II}=\mathcal{N}_{II},\tag{5.37}$$

where P_c is the canonical projection associated with the center-subspace H_c.[5] Thus, assertion (iii) is proved; and the proof is complete. □

The proofs of Theorem 4.3 and Theorem 4.4 are similar to that of Theorem 4.1, and the details are omitted here. For the reader's convenience, we record here the approximation formula for the center manifold function and the reduced equations on the center manifold for each case.

Proof. **(Proof of Theorem 4.3.)** By similar calculation as given above, we can obtain the following approximation formula for the center manifold function:

$$\begin{aligned}\Phi(y,\lambda)=&-\xi_1(\lambda)\gamma_2y^2\cos(\frac{2k_1\pi x_1}{L_1})-\xi_2(\lambda)\gamma_2y^2\cos(\frac{2k_2\pi x_2}{L_2})\\&-\xi_3(\lambda)\gamma_2y^2\cos(\frac{2k_1\pi x_1}{L_1})\cos(\frac{2k_2\pi x_2}{L_2})+o(2).\end{aligned}$$

Here ξ_1, ξ_2 and ξ_3 are given by:

$$\xi_1(\lambda)=\frac{|K_{11}|^2}{16|K_{11}|^4-4\lambda|K_{11}|^2+\sigma},\qquad \xi_2(\lambda)=\frac{|K_{12}|^2}{16|K_{12}|^4-4\lambda|K_{12}|^2+\sigma},$$
$$\xi_3(\lambda)=\frac{|K_1|^2}{16|K_1|^4-4\lambda|K_1|^2+\sigma},$$

where $|K_{11}|^2=\frac{k_1^2\pi^2}{L_1^2}$, $|K_{12}|^2=\frac{k_2^2\pi^2}{L_2^2}$, $|K_1|^2=\frac{k_1^2\pi^2}{L_1^2}+\frac{k_2^2\pi^2}{L_2^2}$.

The reduced equation of (2.6) on the center manifold in this case is:

$$\frac{\mathrm{d}y}{\mathrm{d}t}=\beta_{K_1}(\lambda)y-|K_1|^2\Big(\frac{9}{16}\gamma_3-\big(\xi_1(\lambda)+\xi_2(\lambda)+\frac{1}{2}\xi_3(\lambda)\big)\gamma_2^2\Big)y^3+o(3).$$

□

[5]Here, with a slight abuse of notation, we have identified the two-dimensional center-subspace H_c defined in (5.19) with its coordinate form $\{(y_1,y_2)\in\mathbb{R}^2: y_1e_1+y_2e_2\in H_c\}$.

Proof. **(Proof of Theorem 4.4.)** The center manifold function for this case is:

$$\begin{aligned}\Phi(y,\lambda) = &-\eta_1(\lambda)\gamma_2 y^2\cos(\frac{2k_1\pi x_1}{L_1}) - \eta_2(\lambda)\gamma_2 y^2\cos(\frac{2k_2\pi x_2}{L_2})\\ &-\eta_3(\lambda)\gamma_2 y^2\cos(\frac{2k_3\pi x_3}{L_3}) - \eta_4(\lambda)\gamma_2 y^2\cos(\frac{2k_1\pi x_1}{L_1})\cos(\frac{2k_2\pi x_2}{L_2})\\ &-\eta_5(\lambda)\gamma_2 y^2\cos(\frac{2k_1\pi x_1}{L_1})\cos(\frac{2k_3\pi x_3}{L_3}) - \eta_6(\lambda)\gamma_2 y^2\cos(\frac{2k_2\pi x_2}{L_2})\cos(\frac{2k_3\pi x_3}{L_3})\\ &-\eta_7(\lambda)\gamma_2 y^2\cos(\frac{2k_1\pi x_1}{L_1})\cos(\frac{2k_2\pi x_2}{L_2})\cos(\frac{2k_3\pi x_3}{L_3}) + o(2),\end{aligned}$$

where η_i $(1\le i\le 7)$ are given by

$$\begin{aligned}\eta_1(\lambda) &= \frac{k_1^2\pi^2/L_1^2}{2\big(\frac{16k_1^4\pi^4}{L_1^4} - 4\lambda\frac{k_1^2\pi^2}{L_1^2} + \sigma\big)}, & \eta_2(\lambda) &= \frac{k_2^2\pi^2/L_2^2}{2\big(\frac{16k_2^4\pi^4}{L_2^4} - 4\lambda\frac{k_2^2\pi^2}{L_2^2} + \sigma\big)},\\ \eta_3(\lambda) &= \frac{k_3^2\pi^2/L_3^2}{2\big(\frac{16k_3^4\pi^4}{L_3^4} - 4\lambda\frac{k_3^2\pi^2}{L_3^2} + \sigma\big)}, & \eta_4(\lambda) &= \frac{|K_{12}|^2}{2\big(16|K_{12}|^4 - 4\lambda|K_{12}|^2 + \sigma\big)},\\ \eta_5(\lambda) &= \frac{|K_{13}|^2}{2\big(16|K_{13}|^4 - 4\lambda|K_{13}|^2 + \sigma\big)}, & \eta_6(\lambda) &= \frac{|K_{23}|^2}{2\big(16|K_{23}|^4 - 4\lambda|K_{23}|^2 + \sigma\big)},\\ \eta_7(\lambda) &= \frac{|K_1|^2}{2\big(16|K_1|^4 - 4\lambda|K_1|^2 + \sigma\big)},\end{aligned}$$

with

$$\begin{aligned}|K_{12}|^2 &= \frac{k_1^2\pi^2}{L_1^2} + \frac{k_2^2\pi^2}{L_2^2}, & |K_{13}|^2 &= \frac{k_1^2\pi^2}{L_1^2} + \frac{k_3^2\pi^2}{L_3^2},\\ |K_{23}|^2 &= \frac{k_2^2\pi^2}{L_2^2} + \frac{k_3^2\pi^2}{L_3^2}, & |K_1|^2 &= \frac{k_1^2\pi^2}{L_1^2} + \frac{k_2^2\pi^2}{L_2^2} + \frac{k_3^2\pi^2}{L_3^2}.\end{aligned}$$

The reduced equation of (2.6) to the center manifold is given by:

$$\frac{\mathrm{d}y}{\mathrm{d}t} = \beta_{K_1}(\lambda)y - |K_1|^2\Big(\frac{27}{64}\gamma_3 - \eta(\lambda)\gamma_2^2\Big)y^3 + o(3),$$

where

$$\eta(\lambda) = \eta_1(\lambda) + \eta_2(\lambda) + \eta_3(\lambda) + \frac{1}{2}(\eta_4(\lambda) + \eta_5(\lambda) + \eta_6(\lambda)) + \frac{1}{4}\eta_7(\lambda).$$

□

Appendix A. Dynamic transition theory for nonlinear systems. In this appendix we recall some basic elements of the dynamic transition theory developed by Ma and Wang in [14, 16], which are used to carry out the dynamic transition analysis for the system (2.6) considered in this article.

Let $(H_1, \|\cdot\|_1)$ and $(H, \|\cdot\|)$ be two Hilbert spaces, with $H_1 \hookrightarrow H$ a dense and compact inclusion. Let us consider the following nonlinear evolution equation

$$\begin{aligned}&\frac{\mathrm{d}u}{\mathrm{d}t} = L_\lambda u + G(u,\lambda),\\ &u(0) = u_0,\end{aligned} \tag{A.1}$$

where $u:[0,+\infty)\to H$ is the unknown function and $\lambda\in\mathbb{R}$ is the control parameter of the system. The operators $L_\lambda: H_1\to H$ are a family of linear completely continuous fields depending continuously on λ, which satisfy

$$\begin{aligned} &L_\lambda = -A+B_\lambda && \text{a sectorial operator,}\\ &A: H_1\to H && \text{a linear homeomorphism,}\\ &B_\lambda: H_1\to H && \text{a parameterized linear compact operator.} \end{aligned} \tag{A.2}$$

In particular, L_λ generates an analytic semigroup $\{S_\lambda(t)=e^{tL_\lambda}\}_{t\geq 0}$. Let us also introduce the interpolated spaces H_α as follows. For all $\alpha>0$ one can define fractional powers $(-L_\lambda+a_\lambda I)^{-\alpha}$ of $(-L_\lambda+a_\lambda I)$ for some fixed sufficiently large $a_\lambda>0$; see [14, Sect. 2.2.3]. Note that $(-L_\lambda+a_\lambda I)^{-\alpha}$ is a bounded injective operator on H for each $\alpha>0$. We can then define $(-L_\lambda+a_\lambda I)^{\alpha}$ as the inverse of $(-L_\lambda+a_\lambda I)^{-\alpha}$. The domain of $(-L_\lambda+a_\lambda I)^{\alpha}$, denoted by H_α, is a Banach space under the norm $\|u\|_\alpha := \|(-L_\lambda+a_\lambda I)^\alpha u\|$.

We assume that $G(\cdot,\lambda): H_\alpha\to H$ is a parameterized family of C^r bounded operators for some $0\leq\alpha<1$ and $r\in\mathbb{N}$, which depends continuously on λ. Moreover,

$$G(u,\lambda)=o(\|u\|_\alpha),\quad \forall\ \ \lambda\in\mathbb{R}. \tag{A.3}$$

Let $\{\beta_i(\lambda)\in\mathbb{C}: i\in\mathbb{N}\}$ be the set of eigenvalues of L_λ counting multiplicities, and $\{e_i: i\in\mathbb{N}\}$ be the corresponding eigenvectors which are assumed to be independent of λ. Suppose that the following principle of exchange of stabilities (PES) holds

$$\begin{aligned} &\mathrm{Re}\beta_j(\lambda)\begin{cases} <0, & \text{if } \lambda<\lambda_c,\\ =0, & \text{if } \lambda=\lambda_c, \\ >0, & \text{if } \lambda>\lambda_c, \end{cases} && \forall\ \ 1\leq j\leq m,\\ &\mathrm{Re}\beta_j(\lambda_c)<0, && \forall\ \ j\geq m+1. \end{aligned} \tag{A.4}$$

Now, we recall the following theorem from [16] which provides a basic classification for transitions from equilibrium states of nonlinear systems of the form (A.1). Here, without going into details, we assume that the Cauchy problem (A.1) is well-posed [9], and we can put the model into the perspective of a dynamical system [24], which is indeed the case for many nonlinear systems arising from nonlinear sciences [16].

THEOREM A.1 (Classification of Dynamic Transitions [16, Thm. 2.1.3]). *Consider the system* (A.1). *Assume* (A.2), (A.3), *and the PES condition* (A.4) *hold. Then, the problem* (A.1) *always undergoes a dynamic transition from* $(u,\lambda)=(0,\lambda_c)$, *and there is a neighborhood* $U\subset H$ *of* $u=0$ *such that the transition in* U *is one of the following three types:*

(*i*) **Continuous (or Type-I) Transition**: *there exists an open and dense set* $\widetilde{U}_\lambda\subset U$ *such that for any* $\phi\in\widetilde{U}_\lambda$, *the solution* $u_\lambda(t,\phi)$ *of* (A.1) *with initial datum* $u_\lambda(0,\phi)=\phi$ *satisfies*

$$\lim_{\lambda\to\lambda_c}\limsup_{t\to\infty}\|u_\lambda(t,\phi)\|=0.$$

(*ii*) **Catastrophic (or Type-II) Transition**: *for any* $\lambda_c<\lambda<\lambda_c+\epsilon$ *with some* $\epsilon>0$, *there is an open and dense set* $\widetilde{U}_\lambda\subset U$ *such that for any* $\phi\in\widetilde{U}_\lambda$,

$$\limsup_{t\to\infty}\|u_\lambda(t,\phi)\|\geq\delta>0,$$

where $\delta>0$ *is independent of* λ.

(*iii*) **Random (or Type-III) Transition**: *for any* $\lambda_c<\lambda<\lambda_c+\epsilon$ *with some* $\epsilon>0$, U *can be decomposed into two open (not necessarily connected) sets* U_1^λ *and* U_2^λ*:*

$$\overline{U}=\overline{U_1^\lambda}\cup\overline{U_2^\lambda},\quad U_1^\lambda\cap U_2^\lambda=\emptyset,$$

such that

$$\lim_{\lambda\to\lambda_c}\limsup_{t\to\infty}\|u_\lambda(t,\phi)\|=0\qquad\forall\,\phi\in U_1^\lambda,$$
$$\limsup_{t\to\infty}\|u_\lambda(t,\phi)\|\geq\delta>0\qquad\forall\,\phi\in U_2^\lambda.$$

This theorem shows that as the trivial steady state loses its linear stability, the system (A.1) undergoes a transition of exactly one of the three types. Basically, as the control parameter crosses the critical threshold, the transition states stay in a close neighborhood of the basic state for a Type-I transition, and they go outside of a neighborhood of the basic state for a Type-II transition. For the Type-III transition, a neighborhood is divided into two open regions (not necessarily connected) with a Type-I transition in one region, and a Type-II transition in the other region.

REMARK A.2. It is worth mentioning that the Type-I transition is closely related to the attractor bifurcation [14, Def. 5.1], which includes the classical pitchfork bifurcation as a special case. Assuming (A.2), (A.3), and (A.4), one sufficient condition for the system (A.1) to have an attractor bifurcation at $\lambda=\lambda_c$ is that the trivial steady state is locally asymptotically stable for the system when $\lambda=\lambda_c$; see [14, Thm. 5.2].

For a given dynamical system generated by (A.1), the type of phase transition and detailed dynamical behavior after the transition (at certain critical parameter value) is determined via analysis of a reduced dynamical system on the corresponding center-unstable manifold of the original dynamical system. More specifically, let H_c be the subspace of H spanned by the first m eigenvectors of L_λ with m determined by the PES condition (A.4):

$$H_c:=\text{span}\{e_1,\cdots,e_m\};$$

and H_α^s be the topological complement of H_c in H_α. By the classical invariant manifold theory (see, e.g., [11, Chap. 6] and [14, Thm. 2.12]), under the assumptions (A.2), (A.3), and (A.4), there exists a neighborhood $\mathcal{O}_{\lambda_c}$ of λ_c and a neighborhood U of the origin in H_c, such that the dynamical system generated by (A.1) admits a local center (or center-unstable) manifold $\mathcal{M}_\lambda^{loc}$ near the origin which can be represented as the graph of a function $\Phi(\cdot,\lambda):U\subset H_c\to H_\alpha^s$ for all $\lambda\in\mathcal{O}_{\lambda_c}$. The function Φ is called the center manifold function. We recall that $\mathcal{M}_\lambda^{loc}$ is locally invariant in the sense that any trajectory with initial datum on $\mathcal{M}_\lambda^{loc}$ stays on it and can leave the manifold only from its boundary. Moreover, it attracts exponentially all trajectories of (A.1) that stay within a sufficiently small neighborhood of H_α.

In order to reduce (A.1) to the corresponding local center manifold, we recall that the eigenvectors $\{e_i\,|\,i\in\mathbb{N}\}$ of L_λ and the eigenvectors $\{e_i^*\,|\,i\in\mathbb{N}\}$ of its adjoint operator L_λ^* satisfy $\langle e_i,e_j^*\rangle=\delta_{ij}$ for all $i,j\in\mathbb{N}$, where $\langle\cdot,\cdot\rangle$ is the dual product[6], and δ_{ij} is the Kronecker delta; see [14, Thm. 3.4].

Now, let $u(t,\lambda)=v(t,\lambda)+\Phi(v(t,\lambda),\lambda)$ be a solution on the local invariant manifold, where $v(t,\lambda)=P_cu(t,\lambda)=\sum_{i=1}^m y_i(t,\lambda)e_i\in H_c$. Plugging this expression of u into the

[6]which reduces to the inner product on H when L_λ is self-adjoint.

first equation in (A.1) and taking the dual product with e_i^*, $1 \le i \le m$, on both sides of the equation, we obtain the following reduced system for $y_1(t,\lambda),\cdots,y_m(t,\lambda)$:

$$\frac{\mathrm{d}y_i}{\mathrm{d}t} = \beta_i(\lambda)y_i + \frac{1}{\langle e_i, e_i^*\rangle}\langle G(v+\Phi(v,\lambda),\lambda), e_i^*\rangle, \quad 1 \le i \le m. \tag{A.5}$$

By (A.3), there exists an integer $k \ge 2$, such that the nonlinearity G has a Taylor expansion about $u = 0$ as follows

$$G(u,\lambda) = G_k(u,\lambda) + o(\|u\|_\alpha^k), \tag{A.6}$$

where

$$G_k(\cdot,\lambda) : \underbrace{H_\alpha \times \cdots \times H_\alpha}_{k \text{ times}} \to H$$

is a k-linear operator.

Then, (A.5) can be rewritten as

$$\frac{\mathrm{d}y_i}{\mathrm{d}t} = \beta_i(\lambda)y_i + \frac{1}{\langle e_i, e_i^*\rangle}\langle G_k(v+\Phi(v,\lambda),\lambda), e_i^*\rangle + o(\|\mathbf{y}\|^k), \quad 1 \le i \le m, \tag{A.7}$$

where $\mathbf{y} = (y_1,\cdots,y_m)$ and $\|\mathbf{y}\|$ denotes the Euclidean norm of $\mathbf{y}$ which should not be confused with the norm in H.

In order to obtain an explicit reduced system from (A.7), we need an approximation formula of $\Phi(v,\lambda)$ in terms of v. The following approximation is sufficient for our purpose (see [14, Thm. 3.8]):

$$\Phi(v,\lambda) = (-L_\lambda^s)^{-1} P_s G_k(v,\lambda) + O(|\beta(\lambda)|\|v\|^k) + o(\|v\|^k). \tag{A.8}$$

Here $P_s : H \to H_s$ is the canonical projection into H_s, and L_λ^s is the restriction of L_λ to H_s.

Now, using (A.8) in (A.7) we can obtain an explicit reduced system of m-dimensional ODEs on the local center manifold, which can be used to analyze the local dynamics of the original system (A.1).

Finally, we recall a classical theorem due to A. A. Andronov et al. [1, Chap. IX, Thm. 64], which is very useful in determining the flow structure near the origin of a system of two-dimensional ODEs. This result is used in Section 5 to analyze the reduced equations on the local center manifold.

THEOREM A.3. *Let $P_m(y_1,y_2)$ and $Q_m(y_1,y_2)$ be any given homogeneous polynomials in y_1 and y_2 of order m with $m \ge 1$. Let $\phi(y_1,y_2)$ and $\psi(y_1,y_2)$ be any analytic functions in y_1 and y_2 which are higher order terms with respect to P_m and Q_m as y_1 and y_2 go to zero. Then, any semipath[7] of the analytic system*

$$\begin{aligned} \frac{\mathrm{d}y_1}{\mathrm{d}t} &= P_m(y_1,y_2) + \phi(y_1,y_2), \\ \frac{\mathrm{d}y_2}{\mathrm{d}t} &= Q_m(y_1,y_2) + \psi(y_1,y_2), \end{aligned} \tag{A.9}$$

which tends to the equilibrium state $O := (0,0)$ is either a spiral or tends to O in a definite direction θ^*.

[7]The part of a trajectory of a given ODE system corresponding to either $t \in [t_0,\infty)$ or $t \in (-\infty,t_0]$ if it exists is called a semipath.

If at least one path of the system is a spiral tending to O as $t \to +\infty$ (or as $t \to -\infty$), then all paths passing through points of some neighborhood of O are also spirals (so that O is a stable or an unstable focus).

If $y_1 Q_m(y_1, y_2) - y_2 P_m(y_1, y_2) \not\equiv 0$, the directions θ^* along which the semipaths tend to O satisfy the equation

$$\cos\theta^* Q_m(\cos\theta^*, \sin\theta^*) - \sin\theta^* P_m(\cos\theta^*, \sin\theta^*) = 0. \tag{A.10}$$

Acknowledgement. The authors are grateful to the two anonymous referees for their very detailed and insightful comments, which substantially improved the article. The work was supported in part by the Office of Naval Research and by the National Science Foundation.

REFERENCES

[1] A.A. Andronov, E.A. Leontovich, I.I. Gordon, and A.G. Maier, *Qualitative Theory of Second-order Dynamic Systems* John Wiley & Sons, New York, 1973.
[2] J.W. Cahn, *On spinodal decomposition*, Acta Metallurgica, 9(9), 795–801, 1961.
[3] J.W. Cahn, *Spinodal decomposition*, Tran. Meta. Soc. AIME, 242, 166–180, 1968.
[4] J.W. Cahn and J.E. Hilliard, *Free energy of a nonuniform system. I. Interfacial free energy*, J. Chem. Phys., 28, 258–267, 1958.
[5] A.N. Carvalho, J.A. Langa, and J.C. Robinson, *Attractors for Infinite-Dimensional Non-autonomous Dynamical Systems*, Appl. Math. Sci., Springer, New York, 182, 2013.
[6] R. Choksi, M.A. Peletier, and J.F. Williams, *On the phase diagram for microphase separation of diblock copolymers: An approach via a nonlocal Cahn-Hilliard functional*, SIAM J. Appl. Math., 69(6), 1712–1738, 2009.
[7] R. Choksi and X. Ren, *On the derivation of a density functional theory for microphase separation of diblock copolymers*, J. Stat. Phys., 113, 151–176, 2003.
[8] R.C. Desai and R. Kapral, *Dynamics of Self-organized and Self-assembled Structures*, Cambridge University Press, 2009.
[9] L.C. Evans, *Partial Differential Equations*, Graduate Studies in Mathematics, American Mathematical Society, Providence, RI, 19, 2010.
[10] P.C. Fife, *Models for phase separation and their mathematics*, Electron. J. Diff. Eqs., (48), 1–26, 2000.
[11] D. Henry, *Geometric Theory of Semilinear Parabolic Equations*, Lecture Notes in Mathematics, Springer-Verlag, Berlin, 840, 1981.
[12] C. Hsia, *Bifurcation of binary systems with the Onsager mobility*, J. Math. Phys., 51:063305, 2010.
[13] H. Liu, T. Sengul, and S. Wang, *Dynamic transitions for quasilinear systems and Cahn–Hilliard equation with Onsager mobility*, J. Math. Phys., 53:023518, 31, 2012.
[14] T. Ma and S. Wang, *Bifurcation Theory and Applications*, World Scientific Series on Nonlinear Science. Series A: Monographs and Treatises, World Scientific Publishing Co. Pte. Ltd., Hackensack, NJ, 53, 2005.
[15] T. Ma and S. Wang, *Cahn-Hilliard equations and phase transition dynamics for binary systems*, Disc. Cont. Dyn. Sys. B, 11, 741–784, 2009.
[16] T. Ma and S. Wang, *Phase Transition Dynamics*, Springer-Verlag, 2013.
[17] C.B. Muratov, *Theory of domain patterns in systems with long-range interactions of Coulomb type*, Physical Review E, 66(6), 066108, 2002.
[18] Y. Nishiura and I. Ohnishi, *Some mathematical aspects of the micro-phase separation in diblock copolymers*, Physica D, 84, 31–39, 1995.
[19] A. Novick-Cohen and L.A. Segel, *Nonlinear aspects of the Cahn-Hilliard equation*, Physica D, 10, 277–298, 1984.
[20] T. Ohta and K. Kawasaki, *Equilibrium morphology of block copolymer melts*, Macromolecules, 19(10), 2621–2632, 1986.
[21] L.E. Reichl, *A Modern Course in Statistical Physics*, Wiley-Interscience, New York, 1998.
[22] C. Sagui and R.C. Desai, *Effects of long-range repulsive interactions on Ostwald ripening*, Phys. Rev. E, 52, 2822–2840, 1995.
[23] M. Seul and D. Andelman, *Domain shapes and patterns: the phenomenology of modulated phases*, Science, 267, 476–483, 1995.

[24] R. Temam, *Infinite-Dimensional Dynamical Systems in Mechanics and Physics*, Appl. Math. Sci., Second Edition, Springer-Verlag, New York, 68, 1997.